Cell Proliferation

Cell Prolif., 2014, **47**, 465–475 doi: 10.1111/cpr.12122

Electrospun P34HB fibres: a scaffold for tissue engineering

N. Fu, S. Deng, Y. Fu, G. Li, X. Cun, L. Hao, X. Wei, X. Cai, Q. Peng and Y. Lin

State Key Laboratory of Oral Diseases, West China School of Stomatology, Sichuan University, Chengdu, 610041, China

Received 14-Mar-2014; revision accepted 14-Jun-2014

Abstract

Objectives: Amongst the fourth generation of PHAs is bio-plasticpoly3-hydroxybutyrate4-hydroxybutyrate (P34HB); it is thus appropriate to perform novel research on its uses and applications. The main objective of this study was to determine whether electrospun P34HB fibres would accommodate viability, growth and differentiation of mouse adipose-derived stem cells (mASCs).

Materials and methods: In the present study, we looked at P34HB in two forms, electrospun P34HB fibres and P34HB film. Morphology of electrospun P34HB fibres and P34HB film were characterized using scanning electron microscopy, fluorescence microscopy and confocal laser scanning microscopy, after cell seeding. Cell adhesion, proliferation and cytotoxicity tests were conducted on both by MTT and CCK-8 assays, respectively. After being cultured with osteogenic induction, expression of adipogenic genes *Runx2*, *OPN* and *OCN*, were examined by real-time PCR.

Results: By scanning electron microscopy, light microscopy and confocal laser scanning microscopy, we observed that the mASCs grew well associated with the P34HB materials. After MTT and CCK-8 assay, we concluded that P34HB would, indeed, be a material suitable for further cell adhesion and proliferation studies. More importantly, we found that the P34HB matrices promoted expression of Runx2, OPN and OCN with osteogenic induction.

Conclusions: In this investigation, we can confirm that the electrospun P34HB fibres accommodated survival, proliferation and differentiation of mASCs, and we have been able to draw the conclusion that fibre scaffolds produced by the electrospinning process are promising for application of bone tissue engineering.

Correspondence: Y. Lin, State Key Laboratory of Oral Diseases, West China School of Stomatology, Sichuan University, No. 14., 3rd Sec, Ren Min Nan Road, Chengdu 610041, China. Tel.: +86 28 85503487; Fax: +86 28 85582167; E-mail: yunfenglin@scu.edu.cn

N. Fu and S. Deng contribute equally to this work.

Introduction

Tissue engineering can be recognized as a promising alternative to provision of donor tissues, of which demand often exceeds supply. Although various engineered tissue scaffolds have been developed for tissue substitution, the goal of producing a perfect, clinically useful one, is still far from being realized. An ideal tissue-engineered scaffold should be mechanically stable and capable of complete biologically function at the implant site (1). Electrospun fibres have recently gained substantial interest for such potential applications.

Electrostatic spinning is an interesting method of producing unwoven fibres, with diameters in the range of submicrometres to nanometres. In this process, a continuous filament is drawn from a polymer solution, or 'melts' through a spinneret caused by high electrostatic forces – later to be deposited on a grounded conductive collector (2). Due to high surface area-to-volume ratio of electrospun fibres and high porosity on the submicrometre length scale of nonwoven mats obtained, proposed applications for these materials are in areas such as nanofibre-reinforced composites, nanofibre-based supports for enzyme and catalyst work and nanofibrous membranes. These can be used in many biomedical applications (3–6), including drug delivery, wound healing and scaffolding for tissue engineering. Previous materials for electrostatic spinning have mainly concentrated on PLGA, PCL and more. Few previous studies have investigated the fourth generation of polyhydroxyalkanoates (PHA), namely bio-plasticpoly3-hydroxybutyrate4-hydroxybutyrate (P34HB).

Polyhydroxyalkanoates has a similar structure to various carbon and energy reserve materials, found intracellularly in certain classes of bacteria (7). Due to their appropriate biodegradability and biocompatibility, PHAs

have received considerable attention as environmentally benign plastics, used in a wide range of agricultural, marine and medical applications (8). Earliest research in their field began in the last century. In 1926 in the Pasteur Institute in Paris, France, Lemoigne first discovered and isolated cells from *Bacillus megaterium*, from which could be extracted 3-hydroxybutyrate homopolymer (PHB), the first generation PHA bioplastics. As PHB is brittle, of low elongation at breaking, poor thermal stability though easy processing, little attention had been paid to it; however, in the late 1970s, due to oil crises and environmental protection requirements, PHB began to be examined further. Subsequently, PHA second-generation research, lead to bio-plastic PHBV, and third-generation bio-plastic PHBHHX, were synthesized and properties of the materials were significantly improved. Sadly, there were still flaws. In 1992, the U.S. company Metabolix successfully developed a fourth-generation PHA bioplastics-poly-3-hydroxybutyrate 4-hydroxybutyrate (P3HB4HB or P34HB). Production costs soon dropped, and material properties of P34HB (such as better toughness) also made it a major breakthrough. The Tepha company performed research approved the rate of biodegradation of P34HB can be controlled by varying the 4HB fraction (9) and this copolymer exhibits desirable properties for applications in biomedical and environmental fields (8,10); this has contributed to its increasing research interest from both academia and industry (9,11–17). It overcomes brittleness and the narrow processing window of homopolymer poly-3-hydroxybutyrate (PHB) (18), and has extension from 45 to 100% to break, in accordance with 3–8 mol% 4-hydroxybutyrate (19).

Yet to be a successful implant biomaterial it must meet further requirements such as controllable degradation of the implant and complete integration between native tissues and scaffolds. Degradation products of P3HB4HB based on PHAs are oligo-HAs, including oligo (3-hydroxybutyrate) (OHB) and oligo (3-hydroxybutyrate-co-3-hydroxyhexanoate) (OHBHHx). Previous studies on murine beta cells have directly confirmed that these degradation products have positive effects on cell growth (20). To further advance application of this material, in this study, we have determined capability of P34HB as a suitable electrostatic spinning material for bone tissue engineering.

Mesenchymal stem cells compose a group of multipotent stem cells derived from adult organs and tissues including bone marrow, ligaments, muscles, adipose tissue and dental pulp (21–23). They undergo self-renewal over numbers of generations while retaining the capacity to differentiate into multi-lineage tissues such as bone, cartilage, muscle and fat (24). Even human adipose-derived stem cells (ASCs) are readily available, being relatively easily isolated from elective surgery specimens, such as removal of excess adipose tissue. Some studies have focussed on the similarity between human embryonic stem cell-derived epithelial cells and ameloblast-lineage cells (25), there may also be relationships between ASCs and ameloblast-lineage cells.

Despite these meritorious studies, little effort has been paid to whether P34HB and electrospun P34HB fibres could be a promising scaffold for tissue engineering. Here, our objective was to determine whether electrospun P34HB fibres would accommodate viability, growth and differentiation of mouse adipose-derived stem cells (mASCs).

Materials and methods

Fabrication of polymer scaffolds

With the aid of vortexing overnight, solution of PHA was obtained from suspension of 1.0 g of PHA bio-plasticpoly3-hydroxybutyrate4-hydroxybutyrate (kindly donated by Tsinghua University) in 20 ml organic solvent mixture containing (4:1, v/v) chloroform and dimethylformamide (DMF; Sigma, St. Louis, MO, USA). For the process of electrospinning, polymer solution was placed in a 10 ml glass syringe fitted with a 21G needle to provide a flow rate of 1 ml/h. The syringe was fixed at 45° angle down-tilted from the horizontal. 12–20 kV was applied between the spinneret and the grounded target electrodes; distance between the copper collecting plate (cathode) and needle tip (anode) was 12–15 cm. The polymer solution was drawn from the syringe, forming a pendant drop at the tip of the needle by combination of gravity and the electrostatic charge. A positively-charged jet ejected from the drop was sprayed on the negatively-charged target. Thus a fibrous structure was formed on the collecting plate which was then carefully removed for subsequent use. On the other hand, the P34HB film was obtained simply by placing the polymer solution in a glass dish and allowing evaporation of the volatile liquid. Thickness of both electrospun P34HB fibres and P34HB film were controlled to be 1 mm.

Isolation and culture of mASCs

Four-week-old Kunming mice from the Sichuan University Animal Center, and green fluorescent mice from Sichuan University were used in this study, in accordance with International Guiding Principles for Animal Research (1985). Inguinal fat pads were dissected from the mice and washed extensively in sterile PBS to

remove tissue debris. Fat pads were then digested using 0.075% type I collagenase (Sigma-Aldrich) in PBS, for 60 min at 37 °C, with agitation. After neutralization of collagenase, cells released from specimens were filtered and collected by centrifugation at 1200 ***g*** for 10 min. Resulting pellets were resuspended, washed three times in medium, and cells were seeded in plastic flasks in control medium (α-MEM, 10% FBS). Cultures were maintained in a humidified atmosphere of 5% CO_2 at 37 °C and resultant mASCs were passaged three times prior to differentiation or measurement.

Scanning electron microscopy (SEM)

Electrospun P34HB fibres and P34HB film (which were cut into a rounds to fit well diameter in a 96-well plate, and 1 mm thickness) were placed into 96-well plates. All materials were irradiated under ultraviolet light for half an hour for disinfection purposes. The third passages of green fluorescent mASCs were seeded at an appropriate initial density into the glass-bottomed 96-well plates prepared as described above. After 1, 3, 5 and 7 days cell culture in basic medium, morphology of electrospun P34HB fibres and P34HB film were characterized by SEM (HITACHI S-4800, Tokyo, Japan) equipped with EDS (alpha ray spectrometer, Oxford Instrument, Oxford, UK) at accelerating voltage of 20 kV, prior to and after cell seeding.

Use of green fluorescent mASCs to observe cell growth on matrices

Electrospun P34HB fibres, P34HB film and mASCs in wells of 96 well plates, were prepared as described above. The control group, green fluorescent mASCs were seeded into 6-well plates with no scaffold material, was established. For each group, two parallel rows of wells were set up. After days 1, 5 and 7 culture in basic medium, cells were observed and micrographs were taken, using an Olympus IX 710 microscope (Olympus, Tokyo, Japan).

Confocal laser scanning microscopy (CLSM)

Electrospun P34HB fibres, P34HB film and mASCs in wells of 96 well plates, were prepared as described above. Two paralleled wells were prepared for each group. After seeding green fluorescent mASCs for 7 days, electrospun P34HB fibres and P34HB film were scanned using a laser scanning confocal microscope (LSCM, LEICA TCS SP2; Leica Microsystems, Heidelberg, Germany), by which 3D images were established.

Cell adhesion, proliferation and cytotoxicity testing

Electrospun P34HB fibres, P34HB film and mASCs in wells of 96 well plates, were prepared as described above. A control group of mASCs was seeded into 96-well plates without scaffold materials. For each group, three parallel rows of wells were set up. After 2, 4 and 8 h culture in basic medium, a 3-(4,5-dimethylthiazol-2-yl)-2,5-diphenyl-tetrazolium bromide (MTT) assay was carried out to quantify amounts of viable, cells to determine the extent of cell adhesion on electrospun P34HB fibres and P34HB film. MTT assay is based on the reduction of yellow tetrazolium salt to purple formazan crystals by dehydrogenase enzymes secreted from mitochondria of metabolically active cells. Quantitiy of purple formazan crystals formed is proportional to number of viable cells. First, each culture medium was aspirated and replaced with 200 μl per well MTT solution at 0.1 mg/ml per 96-well culture plate. Secondly, plates were incubated for 4 h at 37 °C. Solution was then aspirated and 150 μl per well dimethylsulphoxide (DMSO) was added to dissolve the formazan crystals. Finally, after 10 min rotary agitation, absorbance of DMSO solution at 570 nm was measured using a Thermospectronic Genesis 10UV/Visible spectrophotometer (Thermo Electron Corp, Madison, WI, USA).

After 1, 3, 5 and 7 days culture in basic medium, cell counting kit-8 (CCK-8) (Dojindo, Kumamoto, Japan) was carried out to quantify viable cells to determine any extent of cell proliferation and cytotoxicity on electrospun P34HB fibres and P34HB film. 10 μl of Cell Counting Assay Kit-8 solution was added to each well and specimens were incubated at 37 °C for 1–4 h to form water insoluble formazan. Then optical density (OD) was measured at 450 nm using a microplate reader (Vari Oskan Flash 3001; Thermo). Amount of formazan dye, generated by activity of dehydrogenases in cells, was directly proportional to number of living cells.

Extraction of total RNA, RT-PCR

RNA was extracted half an hour after seeded the mASCs on the electrospun P34HB fibres and P34HB film; this was followed by culturing with osteogenic induction for 1, 3, 5 and 7 days. We assessed transcriptional levels of *RUNX2*, *OPN* and *OCN* by real-time PCR assay. Initially, total RNA of cells was extracted using Total Tissue/Cell RNA Extraction Kit (Watson, Yunnan, China) according to the manufacturer's protocol. Total RNA (11 μl) was reverse-transcribed into cDNA in a 20 μl reverse transcription system (Fermentas, Vilnius, Lithuania). Total RNA and cDNA of each sample were examined using agarose electrophoresis according to

Table 1. Primer sequences of target genes and GAPDH for real-time PCR assay

Target gene (mouse)	Primer sequence (5′–3′)
Runx2	F: CCGAACTGGTCCGCACCGAC
	R: CTTGAAGGCCACGGGCAGGG
OPN	F: GTGGTGATCTAGTGGTGCCAAGAGT
	R: AGGCACCGGCCATGTGGCTAT
OCN	F: GTCCTATGGCGGGGAGGACTGG
	R: TGGCAGCTGCAAGCTCTCTGTA
GAPDH	F: TATGACTCTACCCACGGCAAGT
	R: ATACTCAGCACCAGCATCACC

protocols outlined in Molecular Cloning: A Laboratory Manual (2001, 3rd edition). cDNA samples were amplified with the aid of an RT-PCR kit (Tiangen, Peking, China) with primers as displayed in Table 1. Expression of specific genes was then quantified using real-time PCR and SYBR Premix Ex TaqTM (Perfect Real Time) kit (Takara, Tokyo, Japan); reactions were carried out on the ABI 7300 system (ABI, Foster City, CA, USA). For each reaction, a melting curve was generated to test primer dimmer formation and false priming, then relative quantification of mRNA levels was carried out by means of double standard curve method. To compare transcription levels of target genes in different quantities of sample, expression of *GAPDH* was used for normalization of real-time PCR results.

Data analysis and statistics

We performed three or more independent sets of experiments, and each experiment was run at least three times. Statistical analysis was performed with SPSS 19.0 (SPSS, Chicago, IL, USA). All data were expressed as mean/standard deviation. Data were analysed by one-way analysis of variance (ANOVA), followed by Student–Newman–Keuls testing; $P < 0.05$ was considered to be statistically significant.

Results

Morphology of electrospun P34HB fibres and P34HB film, prior to and after, mASC seeding

Scanning electron microscopy images of electrospun P34HB fibres and P34HB film prior to cell seeding revealed that the structure of electrospun P34HB fibres was of randomly oriented fibres providing a coarse, porous surface (Fig. 1a), while the structure of P34HB film had no fibres and the surface was relatively smooth and featureless (Fig. 1b). mASCs seeded 1, 3, 5 and 7 days on electrospun P34HB fibres and P34HB film, by SEM showed apparent morphological and qualitative differences (Fig. 2). Seven days after seeding, the mASCs were attached to electrospun P34HB fibres and penetrated into pores between them; numbers of cells were significantly higher (Fig. 2d) compared to mASCs seeded for 1, 3 and 5 days (Fig. 2a–c respectively); 1 day after seeding, cells were somewhat rounded in shape (Fig. 2a), in contrast to more elongated shapes by 7 days after seeding (Fig. 2d). This suggested that the seeded mASCs increasingly attached to electrospun P34HB fibres. Morphology and quantity of mASCs seeded on P34HB film were also remarkable. Seven days after seeding, cells apparently attached to the film and their numbers were significantly higher (Fig. 2h) compared to mASCs seeded for 1, 3 and 5 days (Fig. 2e–g respectively). Whereas the mASCs seeded on electrospun fibres penetrated into interfibrillar pores, those seeded on P34HB film grew on the material surface only.

Morphology of green fluorescent mASCs in electrospun P34HB fibres and P34HB film

Green fluorescent mASCs seeded 1, 5 and 7 days on electrospun P34HB fibres and P34HB film displayed morphological and quantitative differences (Fig. 3). By

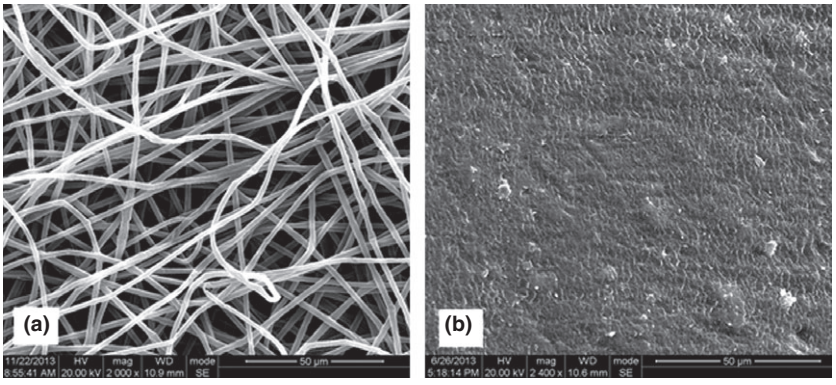

Figure 1. (a) Scanning electron microscopy (original magnification ×2000) of electrospun P34HB fibre structure composed of randomly oriented ultra-fine fibres (bar = 50 μm). (b) Scanning electron microscopy (original magnification ×2000) of P34HB film structure with no ultra-fine fibres (bar = 50 μm).

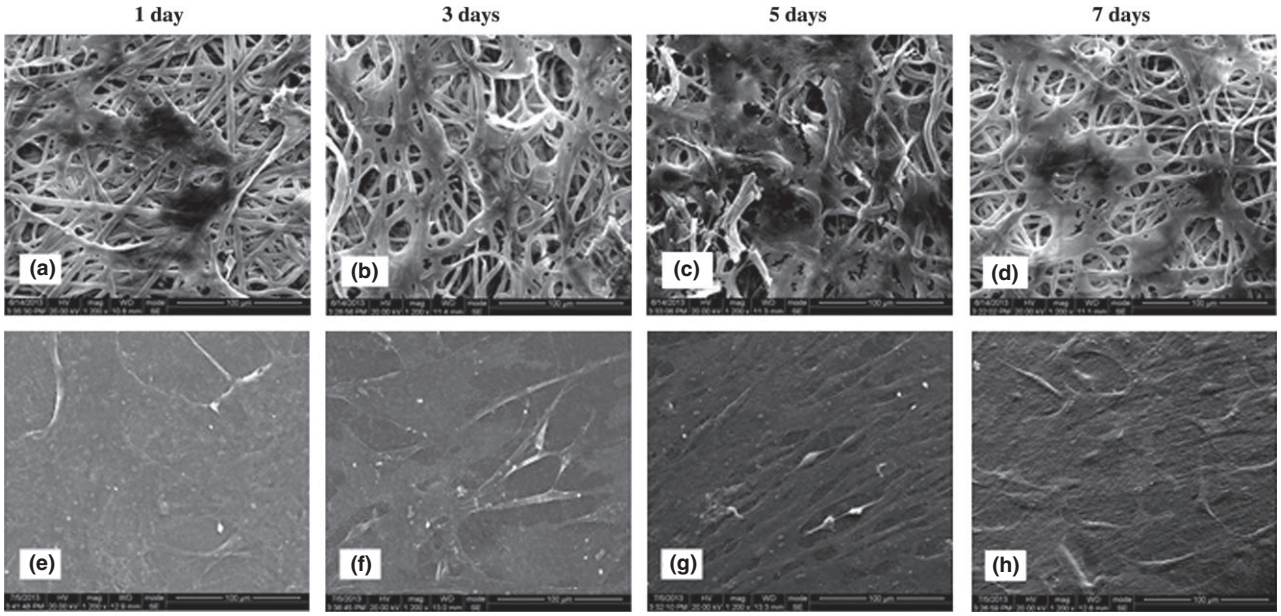

Figure 2. Scanning electron microscopy of morphological and quantitative differences of mouse adipose-derived stem cells after seeding for 1, 3, 5 and 7 days in electrospun P34HB fibres (a–d respectively) and P34HB film (e–h respectively) (scale bar = 100 μm).

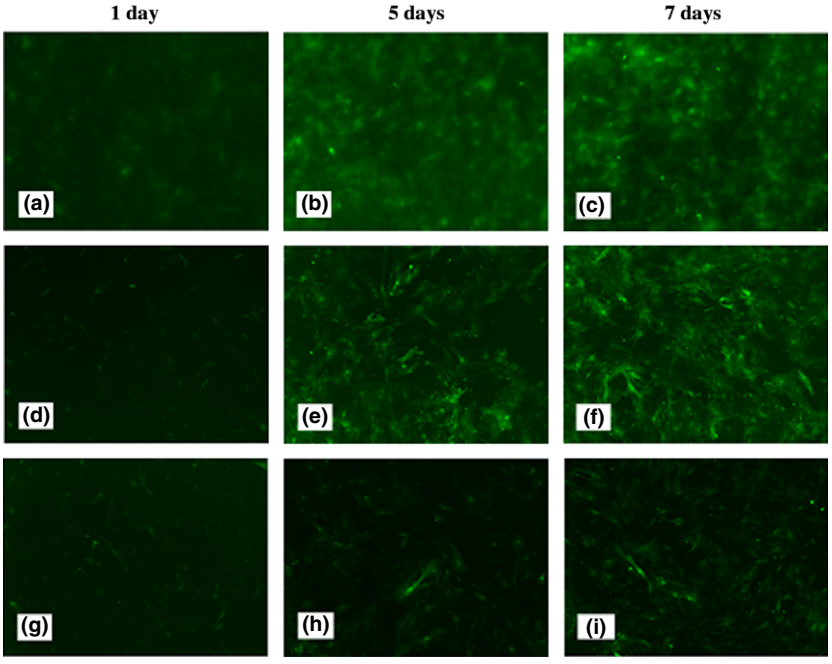

Figure 3. Morphological and quantitative differences in green fluorescent mouse adipose-derived stem cells seeded for 1, 5 and 7 days on electrospun P34HB fibres (a–c respectively) and P34HB film (d–f respectively) (magnification ×100).

5 and 7 days after seeding, the cells attached to the electrospun P34HB fibres and P34HB film, significantly increased in numbers (Fig. 3b,c and e,f respectively), in comparison to the other group (Fig. 3h,i). However, images of electrospun P34HB fibres were successful, although cell numbers could not be determined by assay. Observation however, informed us that the mASCs grew well on P34HB materials.

Image analysis of electrospun P34HB fibres and P34HB film

Confocal laser scanning microscopy was performed to observe morphology of green fluorescent mASCs on electrospun P34HB fibres and P34HB film more closely; Fig. 4 is of flat and 3D images. From the flat 2D image, we can see that compared to P34HB film (Fig. 4b),

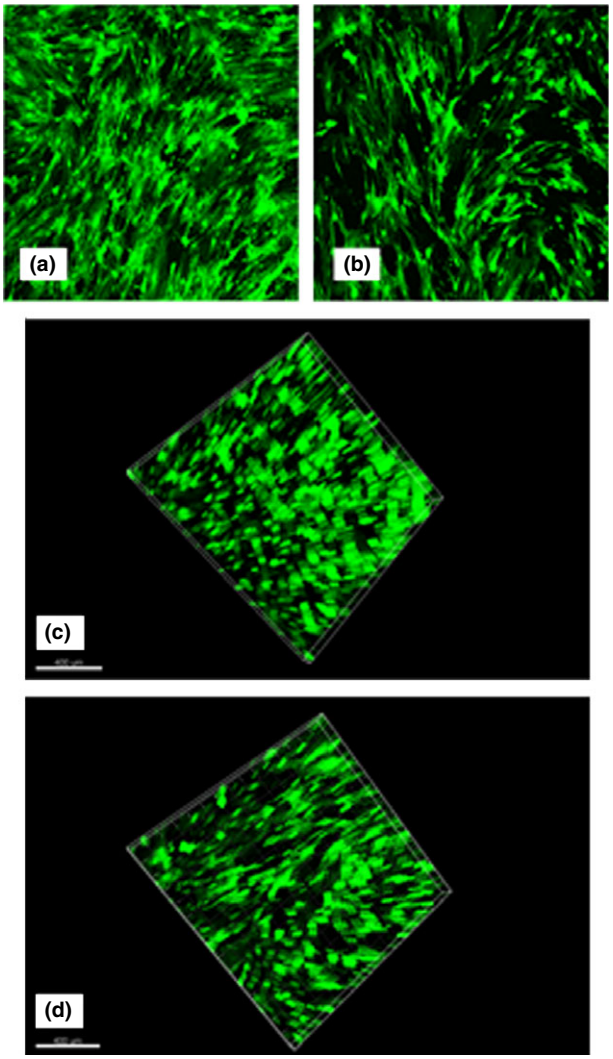

Figure 4. Confocal laser scanning microscopy show the flat (2D) and 3D images of electrospun P34HB fibres (a, c respectively) and P34HB film (b, d respectively) after seeding green fluorescent mouse adipose-derived stem cells for 7 days. Through both 2D and 3D images, we were able to draw the conclusion that mouse adipose-derived stem cells grew well on the P34HB materials (magnification ×100).

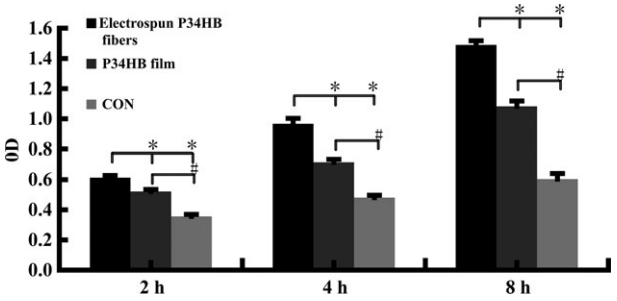

Figure 5. Adhesion test conducted on mouse adipose-derived stem cells on electrospun P34HB fibres and P34HB film. P34HB materials exhibited much greater average absorbance values compared to controls. On the other hand, cells on electrospun P34HB fibres exhibited much greater average absorbance compared to those on P34HB film. $*P < 0.05$ for differences of electrospun P34HB fibres group compared to either the P34HB film group or control group; $\#P < 0.05$ P34HB film group compared to control group.

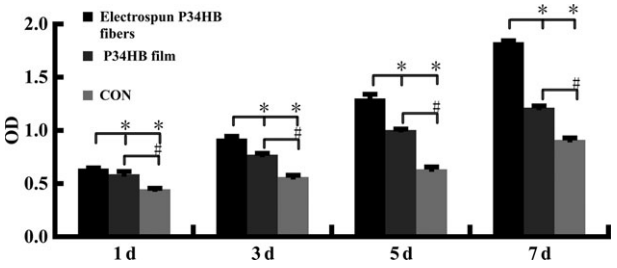

Figure 6. Mouse adipose-derived stem cells on electrospun P34HB fibres and P34HB film cytotoxicity and proliferation were assessed by CCK-8 assay. P34HB materials significantly increased mouse adipose-derived stem cells proliferation. While cells on electrospun P34HB fibres exhibited much greater average absorbance values compared to those of on P34HB film. $*P < 0.05$ electrospun P34HB fibres group compared to either P34HB film group or control group; $\#P < 0.05$ P34HB film group compared to control group.

many more green (live) signals were detected within the electrospun P34HB fibres material (Fig. 4a). By 3D image of electrospun P34HB fibres (Fig. 4c) and P34HB film (Fig. 4d), we detected stronger green (live) signals. Similar to by fluorescence microscopy, green fluorescent cell numbers could not be determined by assay. Thus, once more we were only able to determine that green fluorescent mASCs grew well on the P34HB materials.

Cell adhesion and proliferation, cytotoxicity testing

To determine mASC number by assay, adhesion, proliferation and cytotoxicity tests were conducted on both electrospun P34HB fibres and P34HB film, respectively. Figure 5 shows absorbance obtained from MTT assay, cells with electrospun P34HB fibres or P34HB film having been cultured in 96-well plates in basic medium (in comparison to the cells cultured in 96-well plates without scaffold materials) was established. After 2, 4 and 8 h culture, cells in electrospun P34HB fibres and P34HB film exhibited much greater average absorbance values in compared to controls. On the other hand, electrospun P34HB fibres exhibited much greater average absorbance values compared to P34HB film ($P < 0.05$). Time-dependent mASC proliferation data of the three groups (electrospun P34HB fibre, P34HB film and control) are presented in Fig. 6. After 1, 3, 5 and 7 days culture, electrospun P34HB fibres and P34HB film exhibited much greater average absorbance values in comparison to controls. On the other hand, cells on

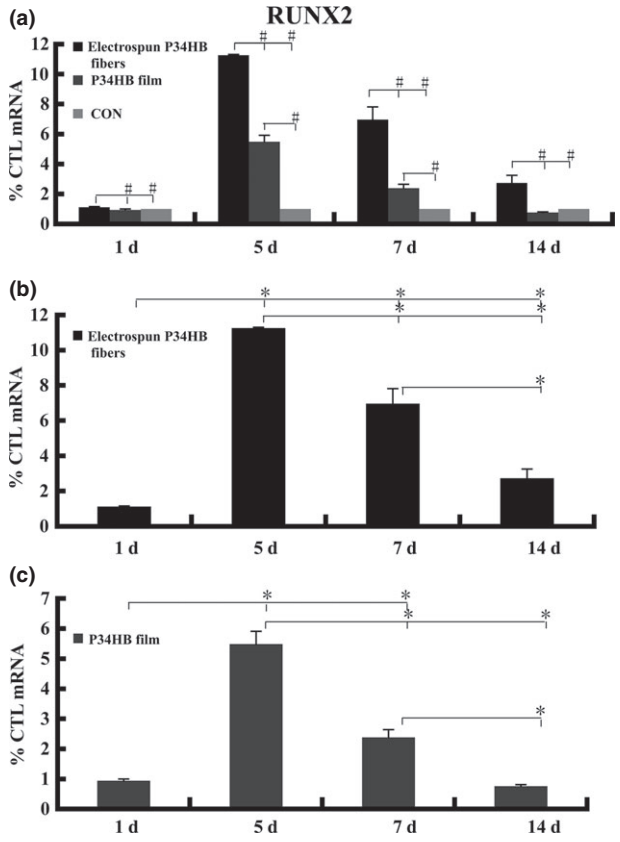

Figure 7. (a) RT-PCR analysis of *Runx2* at different time points; P34HB materials promoted expression of *Runx2* compared to untreated control cultures. *Runx2* expression level of cells on electrospun P34HB fibres was significantly higher than that of those on P34HB film. (b) Significant differences between any two mRNA levels of *Runx2* at four time points of the electrospun P34HB fibres group. (c) Significant differences between any two mRNA levels of *Runx2* at four time points in the P34HB film group. #Comparison between different groups on the same day, *comparison between same groups.

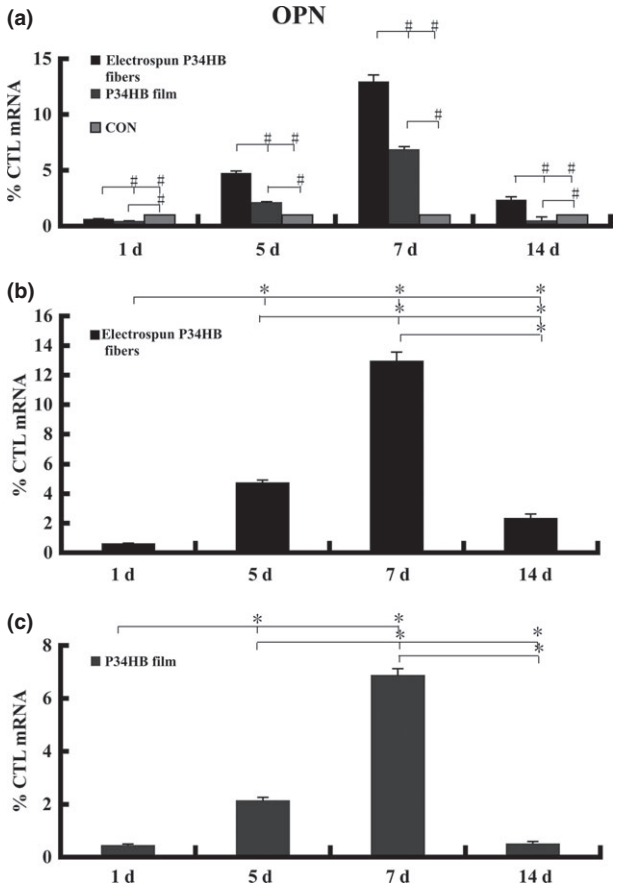

Figure 8. (a) RT-PCR analysis of *OPN* at different time points; P34HB materials promoted expression of *OPN* in cells on them compared to untreated control cultures. *OPN* expression level of electrospun P34HB fibres was significantly higher than that of the P34HB film group. (b) Significant differences between any two mRNA levels of *OPN* at four time points in the electrospun P34HB fibres group. (c) Significant differences between any two of mRNA levels of *OPN* at four time points in the P34HB film group. #comparison between different groups on the same day, and *comparison between same groups.

electrospun P34HB fibres had much greater average absorbance values compared to P34HB film ($P < 0.05$).

P34HB materials promoted expression of Runx2, OPN and OCN with osteogenic induction

After culturing cells for 1, 3, 5 and 7 days with osteogenic induction, mRNA levels of *Runx2*, *OPN* and *OCN* were detected, using real-time RT-PCR (Figs 7,8,9). mRNA levels of *Runx2* in the electrospun P34HB fibres group was significantly higher than those of either P34HB film or control groups. Yet, mRNA levels of *Runx2* in the P34HB film group were significantly higher than the control group, by days 3 and 5; however, there were no significant differences between the P34HB film group and control group on days 1 and 7 (Fig. 7a). For the electrospun P34HB fibres group, there were significant differences between mRNA levels of *Runx2* by days 1, 3, 5 and 7 (Fig. 7b); for the P34HB film group, there were significant differences between mRNA levels of *Runx2* by days 3 and 5 (Fig. 7c). mRNA levels of *OPN* in the electrospun P34HB fibres group were significantly higher than those of either P34HB film group or the control group, by days 1, 3, 5 and 7. On the other hand, mRNA levels of *OPN* in the P34HB film group were significantly higher than in the control group, by days 1, 3, 5 and 7 (Fig. 8a). For the electrospun P34HB fibres group, there were significant differences between mRNA levels of *OPN* by days 1, 3, 5 and day 7 (Fig. 8b); for the P34HB film group, there were significant differences between mRNA levels of

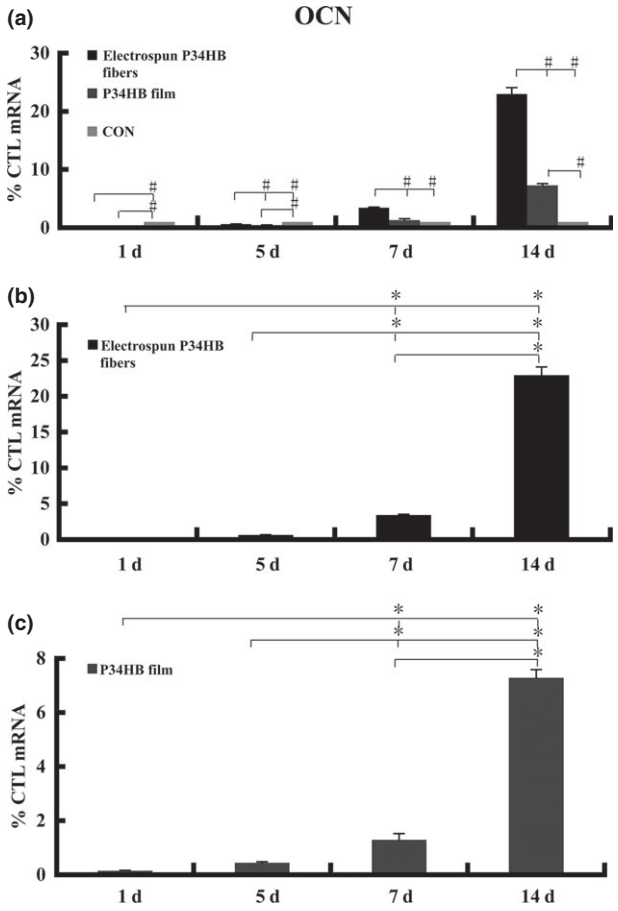

Figure 9. (a) RT-PCR analysis of *OCN* at different time points; P34HB materials promoted the expression of *OCN* compared to untreated control cultures. *OCN* expression level in cells on electrospun P34HB fibres was significantly higher than that of those on P34HB film. (b) Significant differences between any two mRNA levels of *OCN* at four time points, in the electrospun P34HB fibres group. (c) Significant differences between any two mRNA levels of *OCN* at four time points in the P34HB film group. #comparison between different groups on the same day, and *comparison between same groups.

OPN by days 3 and 5 (Fig. 8c). mRNA levels of *OCN* in electrospun P34HB fibres group were significantly higher than those in either the P34HB film group or control group by days 1, 3, 5 and day 7; however, there were no significant differences between electrospun P34HB fibres group and P34HB film group on day 1. mRNA levels of *OCN* in the P34HB film group were significantly higher than the control group by days 1, 3 and 7 (Fig. 9a). For the electrospun P34HB fibres group, there were significant differences between mRNA levels of *OCN* by days 3, 5 and 7 (Fig. 9b) while for the P34HB film group, there were significant differences between mRNA levels of *OCN* by days 3 and 5 (Fig. 9c).

Discussion

The goal of tissue engineering is to furnish living structures that have the potential to integrate with surrounding tissue. Central to formation of newly regenerating tissue is the scaffold which is providing its support. Some previous results have illustrated that adequate bone blood flow is an important clinical consideration, particularly during bone regeneration and in at-risk patient groups (26). The role of the scaffold is to provide anchorage for cells while permitting sufficient bone blood flow. Prior investigations have demonstrated the ability of mineralized bone to form *in vitro* on porous biodegradable polymer scaffolds. A wide variety of scaffold fabrication techniques has been developed, for example, solvent casting/ porogen leaching (27,28), phase separation (29,30), emulsion freeze-drying (31) and gas foaming (32). For treatment of large bone defects, scaffolds should enable blood vessel ingrowth by providing the appropriate architecture and signaling for angiogenesis.

To address effects of scaffold architecture, electrospinning is a promising method for making bone tissue-engineered scaffolds. It is a versatile technique as many different polymers can be processed, and it is simple to set up and operate. The fabrics are highly porous (90%) and provide sufficient space for cell accommodation, allow transport of nutrients and metabolic waste and promote vascular in growth *in vivo*. Because interfibrillar pores are formed by interconnection, there is no need for additional processing steps. The electrostatic spinning technique was first patented in 1934 (2), thus, many of its applications have been studied in different engineering areas. To date, many polymers have been electrospun, including polyethylene oxide (33), acrylic (34), nylon (35), polyethylene glycol, polyac-irylonitrile, polyethylene terephthalate (36), poly(p-phenylene terephthalamide) (37) and more. Seyedmahmoud *et al.* (38) began to characterize mechano-morphological properties of biomaterials for implanted materials and we first fabricated electrospun fibres with P34HB. We further examined biological properties of this material with ASCs.

Previous work in bone tissue engineering has relied on electrospinning, but materials used were mainly concentrated on PLGA (39), PCL (40) and others. Few previous studies simultaneously investigated fourth generation of PHA, namely bio-plasticpoly3-hydroxybutyrate4-hydroxybutyrate (P34HB). The study described here, focusing on P34HB and the P34HB scaffolds, was based on electrostatic fibre spinning. This is consistent with previous work that investigated cytocompatibility of nanofibres (41–43).

Investigative data has shown that P34HB material surface morphology also decides cell viability and growth behaviour (44,45). RaSMCs grew well on all P3HB4HB scaffolds, cells proliferating best on P(3HB-7% 4HB) films and scaffolds (19). There, morphology of electrospun P34HB fibres and P34HB film were characterized using SEM after mASC cell seeding. Micrographs revealed micro observation of cell response to the electrospun P34HB fibres and P34HB film. Results indicated that mASCs attached to the electrospun P34HB fibres and P34HB film and numbers of the cells were high, mASCs penetrating into pores being higher than those on P34HB film. To observe cell morphology more closely on electrospun P34HB fibres and P34HB film, microscopy and CLSM were used to observe green fluorescent mASCs after seeding. We observed them attached to electrospun P34HB fibres and P34HB film in high numbers. However, due to presence of the fibres, cell numbers could not be accurately determined by assay although we were able to observe by and CLSM that mASCs grew well on the P34HB materials.

To determined cell numbers by assay, next cell adhesion, proliferation and cytotoxicity tests were conducted on both electrospun P34HB fibres and P34HB film. Results again showed that P34HB materials were suitable for cell adhesion and proliferation; furthermore, we found that electrospun P34HB fibres had greater advantages over P34HB film.

Reasons for this phenomenon may be the following three points: (i) P34HB materials contain substances, which promote cell proliferation; (ii) surfaces of electrospun P34HB fibres were coarse and porous, while the surface of P34HB film was relatively smooth and featureless. Studies have shown that rough surfaces are conducive to cell adhesion; (iii) electrospun P34HB fibres were woven, providing many pores, thus electrospun P34HB fibres provided high levels of surface area for cells to attach.

Previous data have shown that human AFSCs seeded on scaffolds and cultured in the presence of osteogenic media differentiat towards an osteogenic lineage (46). This has been confirmed by expression of genes associated with mineralization during osteogenesis, including *RUNX2*, *OPN* and *OCN*. *RUNX2* is a key transcription factor associated with differentiation into mature osteoblasts in skeletal development (47). *OPN* and *OCN* expression in bone predominantly occurs in osteoblasts later in the differentiation process, and expression of these factors also has a role in the mineralization process (48,49). In our study, we extracted their mRNA after seeding mASCs on electrospun P34HB fibres and P34HB film, and cultured with osteogenic induction. We found significantly increasing mRNA levels of *Runx2*, *OPN* and *OCN* of mASCs, which suggests that they continued to proliferate upon seeding in P34HB scaffolds. mRNA levels of *Runx2*, *OPN* and *OCN* in the electrospun P34HB fibre group were significantly higher than those of the P34HB film group. This may be because electrospun P34HB fibres scaffold provide a three-dimensional structure for cell attachment, growth and migration, thus promoting expression of *Runx2*, *OPN* and *OCN* in each cell. This speculation warrants experimental investigation and P34HB was chosen as a model polymer due its lack of toxicity.

This study has focused on the electrospinning process for production of P34HB scaffolds and has assessed cell behaviour as an indicator for the potential for bone tissue engineering. Based on the above results, we can conclude that P34HB is a suitable material for cell proliferation and differentiation. Also, we found that electrospun P34HB fibres were better than P34HB film for all performances. Next, we intend to use electrospun P34HB fibres for bone repair in animal experiments.

In conclusion, in this investigation, we confirmed that electrospun P34HB fibres accommodated survival, proliferation and differentiation of mASCs, enabling us to draw the conclusion that P34HB fibre scaffolds produced by the electrospinning process can be introduced for application of bone tissue engineering.

Acknowledgements

This work was funded by the National Natural Science Foundation of China (31170929, 81201211), Doctoral Fund of Ministry of Education of China (20110181120071, 20130181110012) and Funding of State Key Laboratory of Oral Diseases (SKLOD201405).

References

1 Thomson RC, Shung AK, Yaszemski M, Mikos AG (2000) Polymer scaffold processing. *Principles Tissue Eng.* Academic Press, NY, p 251.
2 Formhals A (1934) Process and Apparatus Fob Pbepabing. US Patents 1975504.
3 Kenawy E-R, Bowlin GL, Mansfield K, Layman J, Simpson DG, Sanders EH *et al.* (2002) Release of tetracycline hydrochloride from electrospun poly (ethylene-co-vinylacetate), poly (lactic acid), and a blend. *J. Control. Release* **81**, 57–64.
4 Min B-M, Jeong L, Nam YS, Kim J-M, Kim JY, Park WH (2004) Formation of silk fibroin matrices with different texture and its cellular response to normal human keratinocytes. *Int. J. Biol. Macromol.* **34**, 223–230.
5 Yoshimoto H, Shin Y, Terai H, Vacanti J (2003) A biodegradable nanofiber scaffold by electrospinning and its potential for bone tissue engineering. *Biomaterials* **24**, 2077–2082.

6 Li W-J, Tuli R, Okafor C, Derfoul A, Danielson KG, Hall DJ *et al.* (2005) A three-dimensional nanofibrous scaffold for cartilage tissue engineering using human mesenchymal stem cells. *Biomaterials* **26**, 599–609.

7 Anderson AJ, Dawes EA (1990) Occurrence, metabolism, metabolic role, and industrial uses of bacterial polyhydroxyalkanoates. *Microbiol. Rev.* **54**, 450–472.

8 Chen G-Q, Wu Q (2005) The application of polyhydroxyalkanoates as tissue engineering materials. *Biomaterials* **26**, 6565–6578.

9 Saito Y, Nakamura S, Hiramitsu M (1996) Microbial synthesis and properties of poly (3-hydroxybutyrate-co-4-hydroxybutyrate). *Polym. Int.* **39**, 169–174.

10 Lenz RW, Marchessault RH (2005) Bacterial polyesters: biosynthesis, biodegradable plastics and biotechnology. *Biomacromolecules* **6**, 1–8.

11 Sudesh K, Abe H, Doi Y (2000) Synthesis, structure and properties of polyhydroxyalkanoates: biological polyesters. *Prog. Polym. Sci.* **25**, 1503–1555.

12 Martin DP, Williams SF (2003) Medical applications of poly-4-hydroxybutyrate: a strong flexible absorbable biomaterial. *Biochem. Eng. J.* **16**, 97–105.

13 Zinn M, Witholt B, Egli T (2001) Occurrence, synthesis and medical application of bacterial polyhydroxyalkanoate. *Adv. Drug Deliv. Rev.* **53**, 5–21.

14 Mitomo H, Hsieh W-C, Nishiwaki K, Kasuya K, Doi Y (2001) Poly (3-hydroxybutyrate-co-4-hydroxybutyrate) produced by Comamonas acidovorans. *Polymer* **42**, 3455–3461.

15 Ishida K, Wang Y, Inoue Y (2001) Comonomer unit composition and thermal properties of poly (3-hydroxybutyrate-co-4-hydroxybutyrate)s biosynthesized by Ralstonia eutropha. *Biomacromolecules* **2**, 1285–1293.

16 Zhu Z, Dakwa P, Tapadia P, Whitehouse RS, Wang S-Q (2003) Rheological characterization of flow and crystallization behavior of microbial synthesized poly (3-hydroxybutyrate-co-4-hydroxybutyrate). *Macromolecules* **36**, 4891–4897.

17 Cong C, Zhang S, Xu R, Lu W, Yu D (2008) The influence of 4HB content on the properties of poly (3-hydroxylbutyrate-co-4-hydroxylbutyrate) based on melt molded sheets. *J. Appl. Polym. Sci.* **109**, 1962–1967.

18 Li X-T, Zhang Y, Chen G-Q (2008) Nanofibrous polyhydroxyalkanoate matrices as cell growth supporting materials. *Biomaterials* **29**, 3720–3728.

19 Cheng S-T, Chen Z-F, Chen G-Q (2008) The expression of cross-linked elastin by rabbit blood vessel smooth muscle cells cultured in polyhydroxyalkanoate scaffolds. *Biomaterials* **29**, 4187–4194.

20 Sun J, Dai Z, Zhao Y, Chen G-Q (2007) In vitro effect of oligo-hydroxyalkanoates on the growth of mouse fibroblast cell line L929. *Biomaterials* **28**, 3896–3903.

21 Vats A, Tolley N, Polak J, Buttery L (2002) Stem cells: sources and applications. *Clin. Otolaryngol. Allied Sci.* **27**, 227–232.

22 Turksen K (2004) Revisiting the bulge. *Dev. Cell* **6**, 454–456.

23 Grottkau BE, Purudappa PP, Lin YF (2010) Multilineage differentiation of dental pulp stem cells from green fluorescent protein transgenic mice. *Int. J. Oral Sci.* **2**, 21–27.

24 Le Blanc K, Pittenger M (2005) Mesenchymal stem cells: progress toward promise. *Cytotherapy* **7**, 36–45.

25 Zheng L-W, Linthicum L, DenBesten PK, Zhang Y (2013) The similarity between human embryonic stem cell-derived epithelial cells and ameloblast-lineage cells. *Int. J. Oral Sci.* **5**, 1–6.

26 Tomlinson RE, Silva MJ (2013) Skeletal blood flow in bone repair and maintenance. *Bone Res.* **4**, 311–322.

27 Ishaug SL, Crane GM, Miller MJ, Yasko AW, Yaszemski MJ, Mikos AG (1997) Bone formation by three-dimensional stromal osteoblast culture in biodegradable polymer scaffolds. *J. Biomed. Mater. Res.* **36**, 17–28.

28 Goldstein AS, Zhu G, Morris GE, Meszlenyi RK, Mikos AG (1999) Effect of osteoblastic culture conditions on the structure of poly (DL-lactic-co-glycolic acid) foam scaffolds. *Tissue Eng.* **5**, 421–433.

29 Lo H, Kadiyala S, Guggino S, Leong K (1996) Poly (L-lactic acid) foams with cell seeding and controlled-release capacity. *J. Biomed. Mater. Res.* **30**, 475–484.

30 Saad B, Matter S, Ciardelli G, Neuenschwander P, Suter U, Uhlschmid G *et al.* (1996) Interactions of osteoblasts and macrophages with biodegradable and highly porous polyesterurethane foam and its degradation products. *J. Biomed. Mater. Res.* **32**, 355–366.

31 Whang K, Healy K, Elenz D, Nam E, Tsai D, Thomas C *et al.* (1999) Engineering bone regeneration with bioabsorbable scaffolds with novel microarchitecture. *Tissue Eng.* **5**, 35–51.

32 Harris LD, Kim BS, Mooney DJ (1998) Open pore biodegradable matrices formed with gas foaming. *J. Biomed. Mater. Res.* **42**, 396–402.

33 Jaeger R, Bergshoef MM, Batlle CMI, Schönherr H, Julius Vancso G (1998) Electrospinning of ultra-thin polymer fibers. *Macromol. Symp.* **127**, 141–150.

34 Baumgarten PK (1971) Electrostatic spinning of acrylic microfibers. *J. Colloid Interface Sci.* **36**, 71–79.

35 Gibson P, Schreuder-Gibson H, Rivin D (1999) Electrospun fiber mats: transport properties. *AIChE J.* **45**, 190–195.

36 Warner SB, Buer A, Ugbolue S, Rutledge G, Shin M (1998) A fundamental investigation of the formation and properties of electrospun fibers. *Natl. Textile Center Annu. Rep.* M98-D01, 83–90.

37 Srinivasan G, Reneker DH (1995) Structure and morphology of small diameter electrospun aramid fibers. *Polym. Int.* **36**, 195–201.

38 Seyedmahmoud R, Rainer A, Mozetic P, Giannitelli SM, Trombetta M, Traversa E *et al.* (2014) A primer of statistical methods for correlating parameters and properties of electrospun poly (L-lactide) scaffolds for tissue engineering. I. Design of experiments. *J. Biomed. Mater. Res., Part A* doi: 10.1002/jbm.a.35183, 1552–4965.

39 Xin X, Hussain M, Mao JJ (2007) Continuing differentiation of human mesenchymal stem cells and induced chondrogenic and osteogenic lineages in electrospun PLGA nanofiber scaffold. *Biomaterials* **28**, 316–325.

40 Shin M, Yoshimoto H, Vacanti JP (2004) In vivo bone tissue engineering using mesenchymal stem cells on a novel electrospun nanofibrous scaffold. *Tissue Eng.* **10**, 33–41.

41 Sahoo S, Ouyang H, Goh JC-H, Tay T, Toh S (2006) Characterization of a novel polymeric scaffold for potential application in tendon/ligament tissue engineering. *Tissue Eng.* **12**, 91–99.

42 Katti DS, Robinson KW, Ko FK, Laurencin CT (2004) Bioresorbable nanofiber-based systems for wound healing and drug delivery: optimization of fabrication parameters. *J. Biomed. Mater. Res., Part B* **70**, 286–296.

43 Zong X, Ran S, Kim K-S, Fang D, Hsiao BS, Chu B (2003) Structure and morphology changes during in vitro degradation of electrospun poly (glycolide-co-lactide) nanofiber membrane. *Biomacromolecules* **4**, 416–423.

44 Zhao K, Yang X, Chen G-Q, Chen J-C (2002) Effect of lipase treatment on the biocompatibility of microbial polyhydroxyalkanoates. *J. Mater. Sci. Mater. Med.* **13**, 849–854.

45 Yang X, Zhao K, Chen G-Q (2002) Effect of surface treatment on the biocompatibility of microbial polyhydroxyalkanoates. *Biomaterials* **23**, 1391–1397.

46 Kim J, Jeong SY, Ju YM, Yoo JJ, Smith TL, Khang G *et al.* (2013) In vitro osteogenic differentiation of human amniotic fluid-derived stem cells on a poly (lactide-co-glycolide)(PLGA)-bladder submucosa matrix (BSM) composite scaffold for bone tissue engineering. *Biomed. Mater.* **8**, 014107.
47 Fujita T, Azuma Y, Fukuyama R, Hattori Y, Yoshida C, Koida M *et al.* (2004) Runx2 induces osteoblast and chondrocyte differentiation and enhances their migration by coupling with PI3K-Akt signaling. *J. Cell Biol.* **166**, 85–95.
48 Doherty MJ, Ashton BA, Walsh S, Beresford JN, Grant ME, Canfield AE (1998) Vascular pericytes express osteogenic potential in vitro and in vivo. *J. Bone Miner. Res.* **13**, 828–838.
49 Viereck V, Siggelkow H, Tauber S, Raddatz D, Schutze N, Hüfner M (2002) Differential regulation of Cbfa1/Runx2 and osteocalcin gene expression by vitamin-D3, dexamethasone, and local growth factors in primary human osteoblasts. *J. Cell. Biochem.* **86**, 348–356.

Supporting Information

Additional Supporting Information may be found in the online version of this article:

Video S1. The video S1 shows the 3D image of electrospun P34HB fibers, from the video we can see the green fluorescent cells grow well in the electrospun P34HB fibers, and compare with P34HB film we can detect stronger green (live) signals.

Video S2. The video S2 shows the 3D image of P34HB film, from the video we can see the green fluorescent cells grow well in the P34HB film.